Fully Automatic Road Extraction from SAR Imagery with Bayesian Filter

S. Pourghasemy*, S. Ghofrani*, H.R. Amindavar**

* Electrical Engineering Department, Islamic Azad University, Tehran South Branch, Tehran, Iran.

** Department of Electrical Engineering Amirkabir University of Technology Hafez Avenue, Tehran, Iran

Abstract— **Different techniques have been suggested through time for road extraction from Synthetic Aperture Radar (SAR) images. As for the most efficient, one could mention tracking the points by using the road Bayesian filter. This method uses statistical models to indicate the features of the road. In this paper, Extended Kalman Filter (EKF) is used to extract points located on curved or straight areas and particle filters (PF) to identify the route in the junctions or parts of it which are blocked by a bridge or obstacles of other kind. Moreover, since 1995 during which Bayesian filters have been used, human operator has consistently been of great significance in road extraction and its different stages such as inserting the initial parameter or solving the problem when the algorithm reaches blockages or junctions on its road. However, the advanced world of today endeavors is to decrease the mediation of the man in scientific processes, reduce challenges and progress toward development of technology. The method presented in this paper is faster in processing time in comparison to previous methods by applying Bayesian filters in road extraction process that has been utilized since 1995 for an automated algorithm extracting it from SAR images. Furthermore, to enhance the precision of previously mentioned algorithm, radiometric and geometric features are used simultaneously, hence, more accuracy is achieved over the previous methods.**

Index Terms— extended Kalman filter, particle filter, spoke wheel operator, road map extraction, and synthetic aperture radar

I. INTRODUCTION

Metric analysis radars data such as synthetic aperture radar (SAR) is well known for equipping the accurate information. The new generation of Very High Resolution SAR (VHR SAR) is semi-automatic and it produces commercial outputs for mapping cities, separating waters, monitoring vegetation and extracting roads. Road extraction of satellite images has many applications such as auto-tracking of moving vehicles and positioning roads in time of earthquakes, flood or in general emergency. Research for road extractions of satellite images date back to 1971. In general, the road extraction algorithms are categorized into road detection and network grouping techniques.

Road detection techniques include: edge detection [2], [3], morphological operator [4], intensity cross-section profile matching [5], and road mask filter [7], [8], [9]. The detection techniques recognize the immediate surface of a road, and despite the high-speed processing, they suffer from malfunction road positioning with obstacles (cars), shadows (trees and buildings) and junctions. To overcome the mentioned problem, network grouping techniques such as: Markov random field methods [10], dynamic programming [18] and tracking method [11] were proposed.

One of the most efficient detection technique is point tracking along the road [11]. Where the initial point is tracked by using the primary features and gradually the all points are being tracked along the road. The main advantage of the point tracking method is high speed. In addition, the road extraction is performed by using the knowledge of initial points obtaining at pre-processing stage. An important class of road tracking algorithm is based on the data statistical models and Bayesian estimator. To indicate the features by using the statistical models; two steps named predicting and updating are included. Candidate sample must be predicted at every steps and then updated according to the measurement data.

Bayesian filter [12] has been used for tracking the road points since 1995. In general, a Bayesian filter includes Kalman filter and particle filter (PF). The Kalman filter methodology was first presented in 1995 [12] and later developed in 2006 [6] and 2010 [11]. The PF is a nonlinear filter which uses a single point for tracking [13]. The main drawback of using the Kalman filter [12] or PF [13] is malfunctioning when it reaches severe blockage like existence car on road or junction. The latest theory in the field of road extraction by Bayesian filter was presented in 2010 [11]. This semi-automatic method operates by using the extended Kalman filter (EKF) and the PF.

In this paper, to increase of speed a full automatic method (no needs of human operator) for road extraction of SAR images is proposed. To increase the accuracy, Bayesian filter with feedback as shown in Fig. 1 and explained in detail in Section 3 is used. The pre-processing, including smoothing, Otsu thresholding [20] and morphology filtering, improves the accuracy. The moving spoke wheel operator (SWO) [19] is used to find automatically an initial point, initial angle and road

width. Then, the statistical region growing and hierarchical merging algorithm [17] is used to find automatically the initial gray level of road known as the reference profile. According to some introduced metrics, the proposed algorithm is able to extract 90% of existing roads in a SAR image, and it outperforms other approaches [6], [11], [12] that used Bayesian filter.

The paper is organized as follows. EKF and PF algorithms are reviewed in Section 2. Road tracking method which consists of automatic finding specification of road and road tracking by EKF and PF is explained in Section 3. Time-saving method with high level of accuracy for measuring part of Bayesian filters is also expressed in Section 3. Simulation results conduct on real SAR image road maps are shown in Section 4. Finally, the conclusion is given in Section 5.

The following notations are used in this paper. Boldface lower-case letters (e.g., x) denote vectors, boldface upper-case letters (e.g., **P**) denote matrices. $(.)^T$, $(.)^{-1}$ denote transpose and inverse, **I** and **H** are identity matrices. In addition, f(.) refers to a linear or nonlinear function. Apostrophe indicates the priori state (e.g. $\mathbf{P}'$), and for showing the derivate, we use notation $\dot{\mathbf{x}}$. Meanwhile *N(.), P(.)* and **p(.)** are used for the normal distribution, probability density function, and point coordinate.

II. ROAD MODEL

Using Bayesian filter for road tracking of satellite images requires considering the road median coordinates of an image as a random process and developing a proper discrete state-space model to represent its behavior. The EKF as a processing strategy requires an initial point on the road for starting the operation. The initial point may be set by an operator or through another algorithm. Starting from the initial point, the EKF sequentially proceeds to the next point on the road by using some artificially defined time step. At each step, the process uses the noisy measurement to obtain the best state estimate of the state of the road at that point. Therefore, a stochastic difference equation, referred to as the system equation, is used to model the evolution of a system with the artificial time step,

$$\mathbf{x}_k = f(\mathbf{x}_{k-1}) + \mathbf{v}_k \qquad (1)$$

where $\mathbf{x}_k$ represents the state vector at step *k* and $\mathbf{v}_k$ is the process noise, modeling random variation of the road status from one point to the next. The first model in 1995 used specific parameters stated Vosselman [12]. In general, the system state model of a road is,

$$\mathbf{x}_k = \begin{bmatrix} r_k \\ c_k \\ \theta_k \\ \dot{\theta}_k \end{bmatrix} = \begin{bmatrix} r_{k-1} - dt\sin(\theta_{k-1} + \dot{\theta}_{k-1}dt) \\ c_{k-1} + dt\cos(\theta_{k-1} + \dot{\theta}_{k-1}dt) \\ \theta_{k-1} - \dot{\theta}_{k-1}dt \\ \dot{\theta}_{k-1} \end{bmatrix} + \mathbf{v}_k \qquad (2)$$

where $\mathbf{x}_k$ consist of four parameters (r_k , c_k , θ_k , $\dot{\theta}_k$) as row, column, direction and the road curve or changing the road direction. The system noise $\mathbf{v}_k$ is Gaussian with zero mean and covariance matrix $\mathbf{Q}_k$. Parameter *dt* is the length of moving between two consequent steps (*i.e. k-1* and *k*). The value of *dt* may vary for different steps. Also, other parameters such as the road width or gray level are taken into account as the road features. As the road curve ($\dot{\theta}_k$) in Eq. (2) is assumed not changing all along, an error is occurred. *i.e*. the error of changing the road direction affects the other state variables. In order to consider the error of changing the road direction, the system state equation is updated by using an efficient measurement as follows,

$$\mathbf{z}_k = \mathbf{H}_k\mathbf{x}_k + \mathbf{n}_k \qquad (3)$$

where $\mathbf{z}_k$ is a measurement vector, $\mathbf{H}_k$ is identity matrix with size 4×4, and $\mathbf{n}_k$ is the measurement noise assumed Gaussian with zero mean and the covariance matrix $\mathbf{R}_\mathbf{k}$.

So far, different methods named EKF [11], unscented Kalman filter [15], PF [11], auxiliary particle filter [21], and regulable particle filter [16] were proposed for tracking. In this paper, both EKF and PF are used for tracking a road.

A. Extended Kalman Filter (EKF)

Since the state model of a road is not linear, the linear Kalman filter [12] is not applicable. In contrast, the EKF [11] was developed for nonlinear system and additive noise. Both system and measurement noise ($\mathbf{v}_k$ and $\mathbf{n}_k$) are assumed to be IID(identically independently distributed) Gaussian varies. We also assume that, after local linearization of the nonlinear system, Eq. (1), the priori and posteriori densities are already Gaussian. Furthermore the prior pdf is $P(\mathbf{x}_k \mid \mathbf{z}_{1:k-1}) = N(\mathbf{x}'_{k|k-1}, \mathbf{P}'_k)$ and the posterior probability density function is $P(\mathbf{x}_k \mid \mathbf{z}_{1:k}) = N(\mathbf{x}_{k|k}, \mathbf{P}_k)$. The mean and the covariance matrices are obtained by Kalman filter recursive predicting and updating equations.

Predicting

$$\mathbf{x}'_{k|k-1} = f(\mathbf{x}_{k-1|k-1}) \qquad (4)$$

$$\mathbf{P}'_k = \mathbf{F}_k\mathbf{P}_{k-1}\mathbf{F}_k^T + \mathbf{Q}_k \qquad (5)$$

where $\mathbf{x}'_{k|k-1}$ is a priori state approximation obtained from a nonlinear function of before state specific parameters of Eq. (1) ($f(\mathbf{x}'_{k-1|k-1})$), $\mathbf{P}'_k$ is a priori error covariance matrix at step *k* obtained by system error covariance matrix ($\mathbf{Q}_k$) and priori error covariance matrix at step *k-1* ($\mathbf{P}_{k-1}$) . Meanwhile $\mathbf{F}_k$ is the local linearized function which is obtained through Jacobian [11],

$$\mathbf{F}_k = \begin{bmatrix} 1 & 0 & -dt\cos(\varphi) & -0.5dt^2\cos(\varphi) \\ 0 & 1 & -dt\sin(\varphi) & -0.5dt^2\sin(\varphi) \\ 0 & 0 & 1 & dt \\ 0 & 0 & 0 & 1 \end{bmatrix} \qquad (6)$$

where $\varphi = \theta_{k-1} - \dot{\theta}_{k-1}dt$.

Updating

$$\mathbf{x}_{k|k} = \mathbf{x}'_{k|k-1} + \mathbf{K}_k(\mathbf{z}_k - \mathbf{H}_k\mathbf{x}'_{k|k-1}) \quad (7)$$

$$\mathbf{P}_k = (\mathbf{I} - \mathbf{K}_k\mathbf{H}_k)\mathbf{P}'_k \quad (8)$$

where $\mathbf{x}_{k|k}$ is the optimal point of road which is updated according to the measurements ($\mathbf{z}_k$), $\mathbf{P}_k$ is the Posteriori error covariance matrix obtained according to Kalman gain ($\mathbf{K}_k$) and the priori error covariance matrix ($\mathbf{P}'_k$). The Kalman gain ($\mathbf{K}_k$) at step *k* is

$$\mathbf{K}_k = \mathbf{P}'_k\mathbf{H}_k^{\mathrm{T}}(\mathbf{H}_k\mathbf{P}'_k\mathbf{H}_k^{\mathrm{T}} - \mathbf{R}_k)^{-1} \quad (9)$$

The main disadvantage of EKF is incapability whenever the road state model is not Gaussian, like reaching to a junction. In order to overcome the mentioned problem, the PF explained in following is proposed.

B. Particle Filter (PF)

In general, the PF is used for modeling a nonlinear and non-Gaussian process. The state vector ($\mathbf{x}_k$) for PF is obtained based on the samples ($\mathbf{x}_k^i$) and their weights (w_k^i) as,

$$\mathbf{x}_k = \sum_{i=1}^{L} w_k^i \mathbf{x}_k^i \quad (10)$$

where the state vector $\mathbf{x}_k$ is also named the agent point. To achieve the state vector approximation at the first step, *L* samples are statistically chosen around the initial point considering the normal distribution, then the equal weights are assigned,

$$\mathbf{x}_1^i : N(\mathbf{x}_0, \mathbf{P}_0)$$
$$w_1^i = \frac{1}{L} \quad (11)$$

hereby, $\mathbf{x}_1^i$ is the *i-th (i=1, ... , L)* sample at the first step, $\mathbf{x}_0$ is the initial point, $\mathbf{P}_0$ is the initial error covariance matrix, and w_1^i is the weight of the *i-th* sample at the first step. For the next steps, samples are updated by using the importance density function assumed Gaussian,

$$\mathbf{x}_k^i \sim N(\mathbf{x}_k; f_k(\mathbf{x}_{k-1}^i), \mathbf{Q}_k) \quad (12)$$

where $f_k(\mathbf{x}_{k-1}^i)$ is obtained by using the nonlinear function defined in Eq. (1).

For implementing the PF, samples according to Eq. (12) and the corresponding weights should be obtained. For this purpose, many methods were proposed, in [11] the importance weights are updated up to a normalizing constant by,

$$w_k^i = w_{k-1}^i N(\mathbf{z}_k; h_k(\mathbf{x}_k^i), \mathbf{R}_k) \quad (13)$$

where $h_k(\mathbf{x}_k^i)$ is obtained by using the nonlinear function of Eq. (3). In Section 3, a new method based on the geometric and radiometric features of road for finding the samples weight is proposed.

Eventually, the final prediction of state vector is computed in regards to the updated state and their weights. For finding the prediction of state vector according to Eq. (10 the mean method is used.

Unlike the EKF which is not really suitable for a non-Gaussian state modeling a road junction PF can trace the road states in the case of severe nonlinearity of the system equation or being the non-Gaussian posterior density.

III. Full Automatic Road Tracking via Radiometric and Geometric Features

In this paper, roads are segmented by using the sequential point tracking. As shown in Fig. 1, in general, the road tracking consists of finding the initial values and estimating the dynamic state. The initial values include seed point coordinate, angle for moving on the road, the reference profile, and the road width.

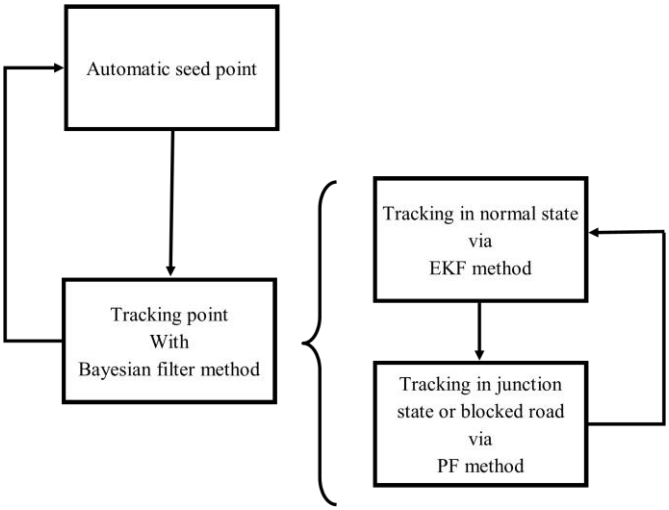

Fig. 1. Tracking using Bayesian Filter

Road may be blocked by shadow of trees, building or the existence of cars due to heavy traffic. Using feedback as shown in Fig. 1 increases the accuracy of road extraction and tracking. Feedback means that the proposed algorithm is able to re-start processing of the first stage and finds the new initial points, though it has already finished the second stage processing. The algorithm goes on tracking the road by using EKF and PF in order to estimate the dynamic state. In addition, it is ended after few iterations (considered 8 iterations) because of trade-off between the processing speed or time consuming and the road segmentation accuracy.

In this paper the full-automatic Bayesian filters for road extraction is used in contrast to being semi-automatic [11], [12]. This means that the initial point, initial width, and initial angle of road for first moving and first gray level of reference profile are obtained automatically. So, the Bayesian processing is going on fast. Furthermore, the radiometric and geometric parameters are used to increase the accuracy.

A. Automatic Finding the Initial Parameters

To indicate the initial features, it is essential to perform pre-processing to heighten quality, contrast, accuracy and processing speed. The following pre-processing are used in this paper:

Laplacian of Gaussian mask (LOG) is used to smooth imagery, promote radiometric features of the road, and a decrease in the gray level variance of the road, see Fig. 2(b).

Canny edge detector is used for positioning the initial coordinates, see Fig. 2(c). Some interested spectral features may be lost if cars or trees exist environs of the road. So using filters to estimate the undesirable spectral affect is necessary. In addition, using pre-processing masks the vegetation, lake, and rivers and speeds up the processing.

(1) Countryside usually has vegetation, trees, mountains, river, and lakes make the edge image being crowded and slow down the process. Otsu method [20] finds the threshold value to remove some excess detected edges.

(2) Opening and closing are two common operation of morphology filters. Opening filter eliminates the small clumps of undesirable foreground pixels, and closing filter removes a small hole on dark image [4].

The output of using the Otsu method and morphology filters is shown in Fig. 2(d).

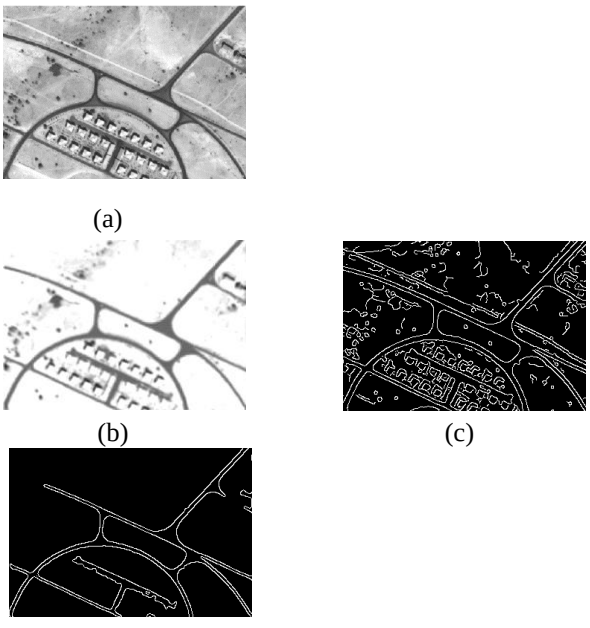

Fig. 2. (a) Quickbird satellite image (b) the output image of using LOG mask (c) image by Canny mask before pre-processing (d) image by Canny mask after pre-processing.

1) Initial Point Coordinate

The main and the first challenge to convert the area of practice from semi- to full- automatic is finding the coordinates of initial point among candidates. In this paper, the initial point is detected via the edge detection image by spoke wheel operator (SWO)**.**

A spoke is a line segment with a length of "m" pixels. A spoke wheel shown in Fig. 3(a) is a sequence of spokes $S_i(\phi_i, m_i)$ $(i = 0, \ldots, 4n-1)$ with common initial point **"p"** and evenly spaced angles. $\phi_i = \pi i / 2n$ [19]. The spoke length, m_i, is the distance between two points where the spoke wheel crosses edges that are locating on two sides. The maximum length of spoke is equal to the maximum road width. It is $b_{\max} = \frac{6 \times 4}{s}$ according to the USA standard road [27], where "s" denotes a SAR image resolution expressed by meter/pixel, 6 is the number of road lane and 4 is the lane width. In general, SWO is moving through the edge image (shown a sample in Fig. 2(d)) and find initial point coordinates automatically, Fig. 3(b).

Although the detected edge point is assumed to be the road point, it might belong to a building, vehicle or trees within the edge image. To assure about, the 8-neighbors around the candidate point are considered. If there is another edge point, they both are assumed as the road edge. If no point or more than one point is found, candidate point is eliminated and searching to find the candidate point is continued. After that, the angle between these two candidate points is supposed as the movement angle for finding the road line. We move around the last detected point according to the angle and with a hypothetical threshold named T_a and assumed 0.2rad, moreover moving step (dt), also we repeat the procedures in case a new edge point is found. For SAR images, the minimum road length is assumed $l_{\min} = mbl / s$ where mbl the maximum of building length which assumed 30 meters is. According to the number of located points, the length of candidate line as shown in Fig. 3(c) is obtained. If the length of candidate line is greater than $l_{\min}$, then Algorithm 2 starts. If the length of candidate line is less than $l_{\min}$ and another point is not found, then Algorithm 1 is run again. It means that the candidate point is declined, another candidate point is chosen, and the candidate line is obtained and go on.

Algorithm 1 Find line from detected edge image

detected edge image ¬ canny edge detector

$\mathbf{p}(r_1 , c_1)$ ← find first point by use of detected edge image

$\mathbf{p}(r_2 , c_2)$ ← Put 3×3 mask on first point and find second point by use of detected edge image

hypothetical angle $= \tan^{-1}(\frac{r_2 - r_1}{c_2 - c_1})$

line length $= l_{\min}$

$j = 2$

while line length **do**

for angle = hypothetical angle $-T_a$ to hypothetical angle $-T_a$ **do**

$prob\ row = r_j - dt \sin(angle)$

$prob\ coloumn = c_j + dt \cos(angle)$

if (prob row , prob column) is on the edge point

then :

$j = j + 1$

$\mathbf{p}(r_j , c_j) = (prob\ row , prob\ column)$

break

end if

end for

line length = line length-1

if do not detected any point on the edge **then** :

$j = 1$

Go to stage one and search again for finding first point of candidate line

break

end if

end while

In order to find the adjacency parallel line, $\mathbf{pl}_a$, we return to the first candidate point, $\mathbf{pl}_m(r_1 , c_1)$, place SWO on it and search for another edge point in interval $[180^o \ \ 180^o - T_a]$ or $[0 \ \ T_a]$ angle, (see Fig. 3(d)). If no point is found, the Algorithm 1 re-starts to find another initial point. If more than one point is found, the point with the least spoke length is chosen (see Algorithm 2). For obtaining the adjacency road line, the same steps explained as Algorithm 1 for the main road line took part.

Algorithm 2 Find first adjacent point

Put spoke wheel ($S_i(\phi_i , m_i)$) on the first candidate point

$\mathbf{p} = \mathbf{pl}_m(r_1 , c_1)$

$m_i =$ distance between "$\mathbf{p}(r,c)$" and place that i th spoke cuts the edge

for $j = 1$ *to* $4n - 1$ **then** :

if spoke which it doesn't cut any edge

eliminate $\mathbf{S}_j(\phi_j , m_j)$

end if

end for

min length of spoke $= b_{\max}$

for $j = 1$ *to* $4n - 1$ **then** :

if $m_i <$ min length of spoke **then** :

min length of spoke $= m_i$

row and column which it is cut by i th spoke

↓

hypothetical adjacency candidate point

end if

end for

$\mathbf{pl}_a(r_1 , c_1) =$ hypothetical adjacency candidate point

In general, a road is defined in terms of two parallel line, so the distance between two lines are not changing. Algorithm 3 double checks the distance. It computes the distance between every points of two located lines as shown in Fig. 3(e), if a distance less than $b_{\max}$ is found, the candidate road line and the candidate adjacency road line are supposed to be true. The Algorithm 1 successfully ends if the length of adjacency line is more than $l_{\min}$, and initial road line is located.

Algorithm 3 Check adjacency point

p ← founded point for adjacency candidate line
N ← number of founded point in candidate line
for $i = 1$ *to* N **do**:
  d_i ← distance between **p** and $\mathbf{pl}_m(r_i, c_i)$
  if $d_i < b_{\max}$ **then**:
    founded point is true
  end if
end for
  if all distance is bigger than $b_{\max}$ **then**:
  candidate adjacency line is outside of road width range and we should go to Algorithm 1 and search again
end if

point for each cluster according to samples and their weight, (h) updating samples and repeat algorithm.

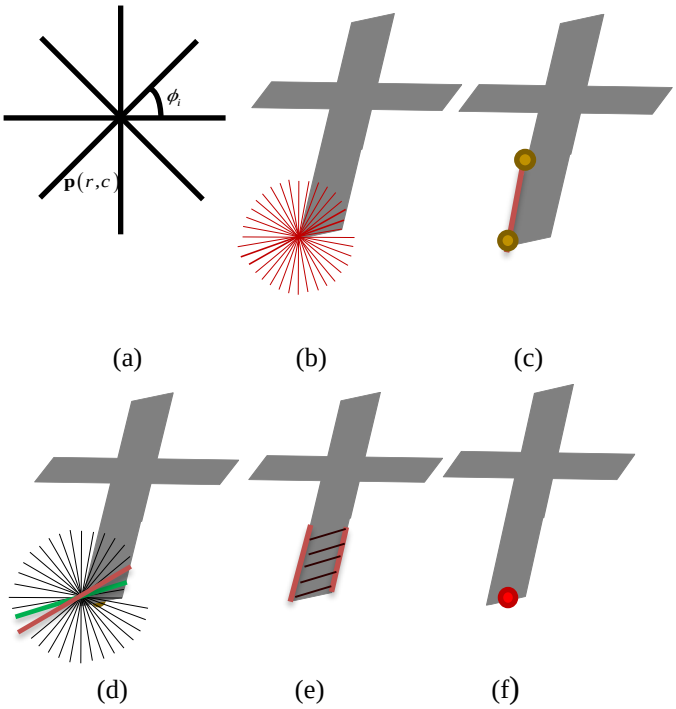

Fig. 3. (a) Spoke wheel, (b-f) process of initial point finding.

Ending successfully the Algorithms 1, 2, and 3 means that the initial point coordinate of the road line and the adjacency parallel line are obtained. Accordingly, as a sample point is seen in Fig. 3(f), the initial mid-point coordinate is computed. Furthermore the initial road width, b_{init}, according the first point of main and adjacency road line, and the initial angle of road direction, a_{init}, according to main road line are obtained (see Fig.4),

$$b_{init} = \left|\mathbf{pl}_m(r_1,c_1) - \mathbf{pl}_a(r_1,c_1)\right|^2 \quad \times \quad s$$
$$a_{init} \;=\; \text{median}\left(\; \varphi_i|_{i=1}^{N} \;\right) \qquad (14)$$

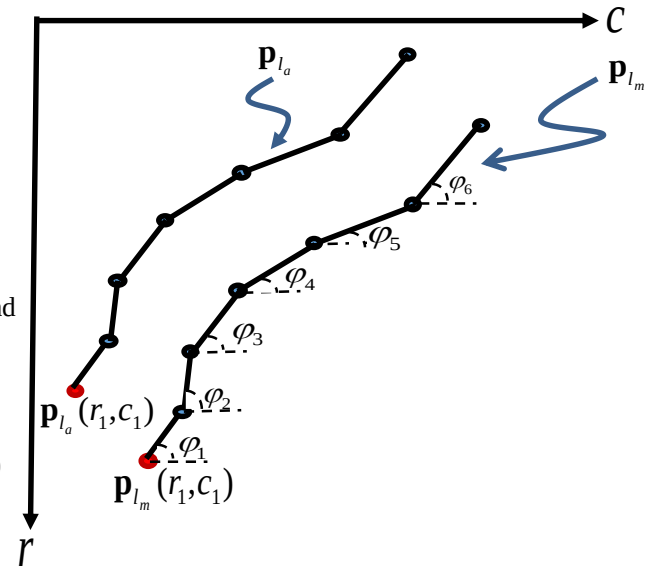

Fig. 4. Candidate and adjacency candidate line.

2) Automatic Find Reference Profile

Reference profile, which is used in measurement stage, refers to the road gray levels. In order to find the reference profile, as shown in Fig. 5, the output image of LOG mask is used. The directional mask with size $5b_k \times 5b_k$ is placed on the intended road point according to the estimated angle of this point, see Fig. 5(c). Where b_k is the road width obtained according to distance between two edge of parallel line of the road in position of point on *k*-th step. Then the Otsu threshold [20] is obtained. Assuming that a road is dark in comparison with other image components, all pixels with gray levels greater than the Otsu threshold value are modified to 255. Simply, they do not contribute to obtain the road reference profile. The pixels located inside the directional mask with gray levels less than Otsu threshold are now classified according to the statistical region growing and hierarchical merging algorithm [17], and a class with the most number of pixels is known as the reference profile candidate. For this purpose, the coefficient variable, *cv*, is obtained,

$$cv = \frac{\sigma_t}{\bar{t}} \qquad (15)$$

where σ_t and $\bar{t}$ are the standard deviation and the mean value of all pixels belong to the directional mask $5b_k \times 5b_k$ and also with intensity less than the Otsu threshold. Moreover these

pixels, in general, are named t. At first iteration, the number of classes are the same as the number of pixels that are inside the directional mask with gray levels less than Otsu threshold. In continuing, two neighbor classes may merge if cv ≤ T is satisfied,

$$T = \sigma_c (1 + \eta \sqrt{\frac{1 + 2\sigma_c^2}{2L}}) \quad (16)$$

where L is the total number of pixels belong to the two classes (named region process) that may be merged, η experimentally set to 0.075. We assume that two classes is merged and to prove our claim, all pixels of adjacent class is inserted into candidate class, so region process is formed, and σ_c denotes the standard deviation of the region process. Under satisfaction $cv \leq$ T, the new class of inserting pixels are merging two old classes is accepted. The statistical region growing is continued until there are no more similar classes to merge.

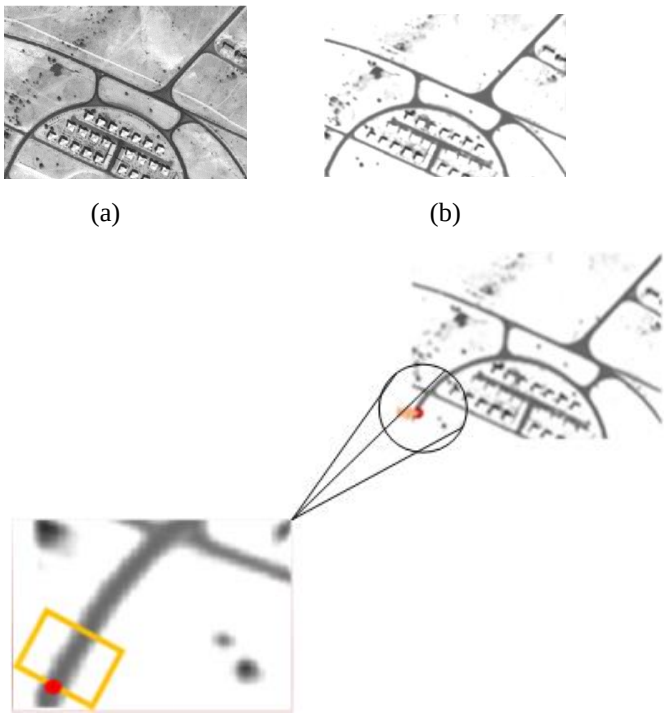

(a) (b) (c)

Fig. 5. (a) Quickbird satellite image (b) output image of LOG mask (c) using the directional mask with size $5width \times 5width$.

Among all candidate classes as the reference profile, a class with maximum L or maximum number of pixels is chosen. Then, according to the estimated road width in Eq. (14), b_k , and image resolution, s, the length of reference profile or the number of gray levels, L_{rpf} , is obtained,

$$L_{rpf} = \frac{b_k}{4s} \quad (17)$$

The number of L_{rpf} pixels with maximum repetition in terms of gray levels are considered as the reference profile, see Algorithm 4.

Algorithm 4 Automatic reference profile finding

thresh ← Otsu threshoulding
region process ← put directional mask on initial point according to initial obtained angle
L ← region process length
for i = 1 to L **do**:
if gray level of region process (i) > thresh **then**:
gray level of region process (i) = max gray level
end if
end for
cluster(i) ← merge elements of region process by use of statistical region growing and hierarchical merging algorithm
L ← number of cluster
for i = 1 to L **do**:
if length of cluster(i) >Max length of cluster **then**:
Max length of cluster = length of cluster(i)
chosen cluster = cluster(i)
end if
end for
$L_{rpf} = \frac{b_k}{4s}$
for i = 1 to length of reference profile **do**:
reference profile ← element of chosen cluster which it has maximum repeat
end for

B. Road Tracking

After indicating the primary features of the road, including the initial point coordinates, angle, width and the initial reference profile (Algorithms 1-4), the EKF and PF as Bayesian or recursive filters use the information to track the road points.

The objective is realizing the posteriori state vector of the road by using the all available information which should be a comprehensive collection of perceived measurements. At many occasions, a new estimation of the system is required for every new measurement. In such circumstances, the Bayesian filter [12] because of processing the input data sequentially and no need to process all pixels of an image is a great asset. The capability of sequentially processing in recursive filters make them run fast. The Bayesian filter consists of two main stages; predicting and updating. In general the prediction stage is

erroneous because system status is affected by undetermined turbulence modeled as random noise. Using measurements, the predicted point is updated by Bayesian rule as a mechanism for updating the target status.

1) Extended Kalman Filter

As mentioned before, the EKF is a nonlinear filter and is able to estimate a Gaussian posteriori density. It uses the obtained initial point for predicting the next point coordinate (refer to Eqs. (4), (5)). Since the changes of the road angle is assumed constant, and due to undesirable errors, the optimal measuring, which will be explained in Section 3.3, is of high essence. Through measurements, the previous prediction is updated with minimal occurrence of errors (refer to Eqs. (7), (8)).

So far, a variety of techniques have been introduced to decrease the measurement error, though they have drawbacks. For instance, the proposed method by Vosselman [12] depends on road direction and its changes. In addition, the proposed method by Movaghati [11] depends on the road gray levels of reference profile. So, the measurement error is occurred for low resolution SAR images where the road homogeneity is less or the road gray levels variance is high. In this paper, both geometric features (road edge images) and radiometric features (road gray level) are used to overcome the above mentioned drawbacks (see Section 3.3).

2) Particle Filter

When EKF reaches a blocking area like vehicles, and bridge, it cannot continue tracking because no new point is found. So, the procedure of road tracking is continued by PF. Especially EKF may reaches a crossroad which is found according the following procedures.

(1)- Consider a spoke wheel with spoke angle equal, $\phi_i = \pi i / 2\times 60$. Localize the spoke wheel with different spoke length on the last point found by EKF. It was mentioned earlier, the spoke length comes along the intended point to the road edge. It is considered to be b_k if the spoke wheel does not cross any road edge.

(2)- Keep the spokes with maximum length b_k and remove other spokes.

(3)- Compute the angle between two consecutive spokes. If the angle is greater than 0.5 radian, it shows a road branch. And this procedure is repeated for other consecutive spokes.

(4)- At last, due to the fact that crossroads have three or more road branch, if three or more road branch is found, supposed that a crossroad is found.

In general, the PF starts tracking by using the last point found by EKF, $\mathbf{x}_k$ (Eq. (7)), the error covariance matrix, $\mathbf{P}_k$ (Eq. (8)), and considering the Normal distribution. At first sample points around $\mathbf{x}_k$ are chosen (Eq. (11)), then some of them are discarded by considering the reference profile. The Measurements (explained in Section 3.3) of every sample is obtained and they are clustered by using [26], according to the angle between agent point ($\mathbf{x}_k$ at first iteration) and intended measurement, φ_m , and the threshold value, T_a. In order to correspond each sample, $\mathbf{x}_k^i (i = 1, \ldots, L)$, into one of M clusters, $\mathbf{z}_m$ $(m = 1, \ldots, M)$, the Mahalanobis distance among every measurements and each samples are obtained,

$$d_{i,m} = (\mathbf{z}_m - h_k(\mathbf{x}_k^i))^T \mathbf{R}_k^{-1} (\mathbf{z}_m - h_k(\mathbf{x}_k^i)) \tag{18}$$

where $d_{i,m}$ is the Mahalanobis distance between *i-th* sample ($\mathbf{x}_k^i$) and *m*-th measurement ($\mathbf{z}_m$) data and $\mathbf{R}_k$ is the measurement error covariance matrix. The *i-th* sample is assigned to that cluster with minimum Mahalanobis distance.

As seen in Eq. (10), implementing the PF needs obtaining the weighting factors. For this purpose, three parameters explained in following are used by considering the road radiometric and geometric features.

The first parameter is proximity weight which is proximity of *i-th* sample to m-th measurement cluster and it is calculated via Mahalanobis distance (refer to Eq. (18)) as,

$$\overset{\circ}{w}{}_M^i = w_{prev}^i \frac{1}{(2\pi)^{D/2} \left|\mathbf{R}_k\right|^{1/2}} \exp\left[-\frac{d_{i,\mathrm{j}}}{2}\right] \tag{19}$$

$$w_M^i = \frac{\overset{\circ}{w}{}_M^i}{\sum_{i=1}^{N} \overset{\circ}{w}{}_M^i} \tag{20}$$

where D = 3 is the dimension of the measurement vector, $\mathrm{d}_{\mathrm{i,j}}$ is the least value of Mahalanobis distance, w_M^i is proximity weight of *i-th* sample, and w_{prev}^i is previously weight of *i-th* sample which assumed $1/\mathrm{L}$ at the first iteration.

The second parameter is similarity weight which is similarity of reference profile, **rpf** , and sample profile, **spf** .

$$\begin{aligned} \overset{\circ}{w}{}_G^i &= 1 - e \\ w_G^i &= \frac{\overset{\circ}{w}{}_G^i}{\sum_{i=1}^{N} \overset{\circ}{w}{}_G^i} \end{aligned} \tag{21}$$

where gray level error, *e*, is equaled as follow,

$$\left.\begin{aligned} r &= \frac{\mathrm{cov}(\mathbf{rpf}, \mathbf{spf})}{\mathrm{var}(\mathbf{rpf}).\mathrm{var}(\mathbf{spf})} \qquad e_1 = l - r \\ e_2 &= \left\{ \frac{\left| mean\{\mathbf{rpf}\} - mean\{\mathbf{spf}\} \right|}{mean\{\mathbf{rpf}\}} \right\}^2 \end{aligned}\right\} e = \frac{e_1 + e_2}{2} \tag{22}$$

rpf is gray levels of reference profile, also gray levels of sample profile, **spf** , is vertical line gray level which it put on *i-th* sample according to angle between *i-th* sample and agent point,

The third parameter is angular deviation,

$$w_A^j = 1 - \theta_d \tag{23}$$

where $\theta_d = \min(\theta_1, \theta_2)$, $\theta_1 = \dfrac{\left|\theta_k^i - \theta_{agent}\right|}{\theta_{agent}}$, $\theta_2 = \dfrac{\left|(180 - \theta_k^i) - \theta_{agent}\right|}{\theta_{agent}}$,and $\theta_k^i = \tan^{-1}(\dfrac{r_k^i - r_{agent}}{c_k^i - c_{agent}})$. The pairs (r_k^i, c_k^i) , and (r_{agent}, c_{agent}) refer to the *i-th* sample at step *k* and agent point coordinates. The angular deviation is the angle between the *i-th* sample and agent point, both belong to the same cluster.

Now, the weighting factor, w_k^i , for *i-th* sample at step *k* is determined,

$$w_k^j = \alpha w_M^j + \beta w_G^j + \gamma w_A^j \tag{24}$$

where $\alpha + \gamma + \beta = 1$, and $\alpha < \gamma < \beta$. Then, the agent point named $\mathbf{x}_{agent}$, for every cluster is obtained,

$$\mathbf{x}_{agent} = \sum_{i=1}^{L} w_k^i \mathbf{x}_k^i \tag{25}$$

At the end, samples of each cluster are updated,

$$\mathbf{x}_k^i \sim N(\mathbf{x}_{agent}; f_k(\mathbf{x}_{k\text{-}1}^i), \mathbf{Q}_k) \tag{26}$$

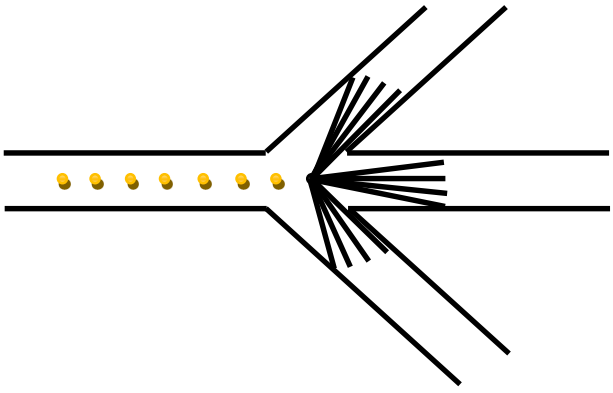

(a)

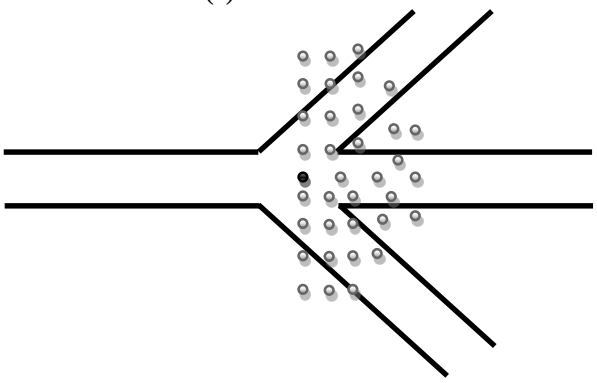

(b)

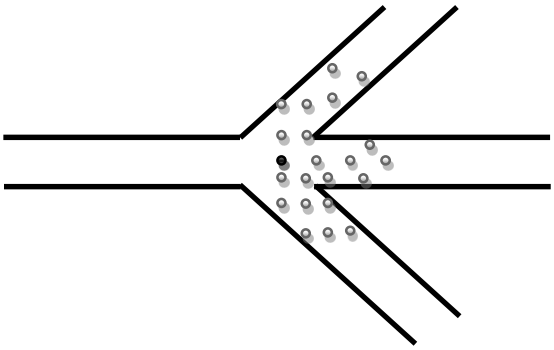

(c)

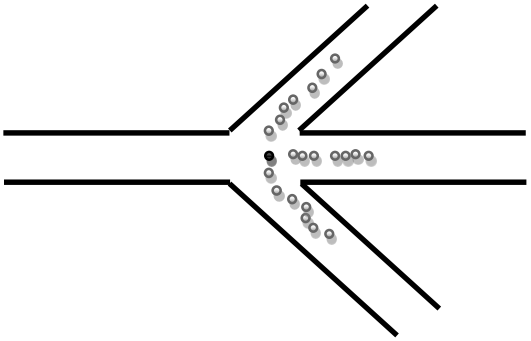

(d)

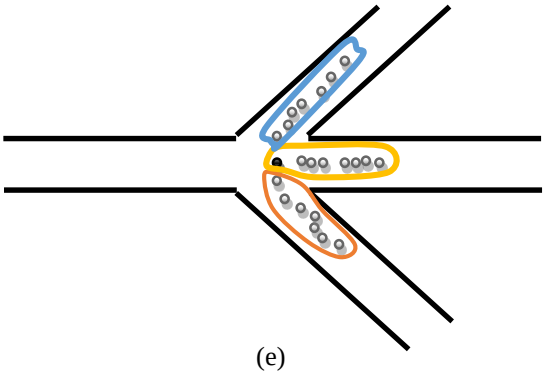

(e)

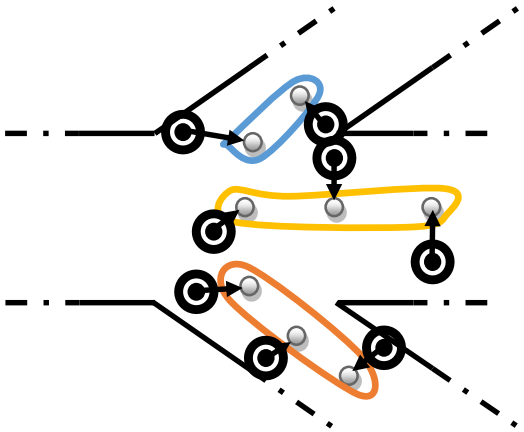

(f)

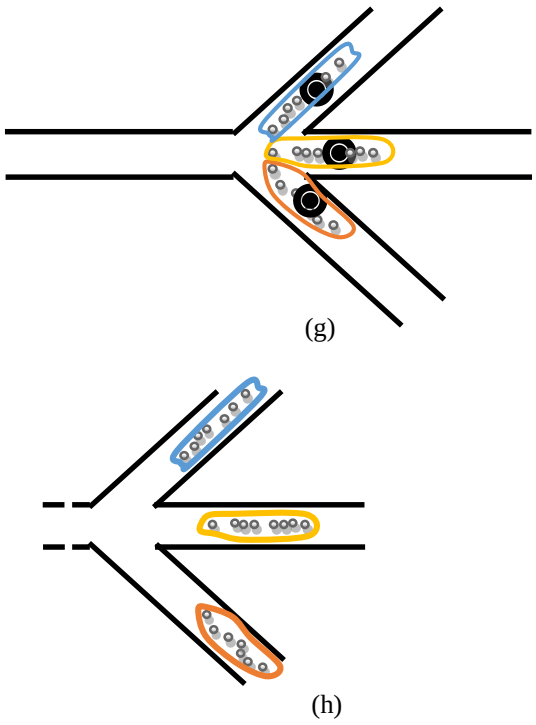

Fig.6 . Particle filter (a) cross road detected, (b) sampling around last point of EKF, (c) eliminate non road point, (d) measuring, (e) clustering measurement, (f) assigning samples to proper measurement cluster, (g) equal agent point for each cluster according to samples and their weight, (h) updating samples and repeat algorithm.

In this paper, PF switches to EKF after 8 iteration. The EKF uses the last sample points found for every clusters.

At the end, when both EKF and PF are not able to find a new point, as feedback shown in Fig. (1), the algorithm attempt to find a new point to track in the imagery. If a new initial point is found, stage 2 from algorithm is repeated. To define a trade-off between the speed and accuracy of the process, the algorithm after several repetitions is ended (8 iteration).

C. Measurement

As mentioned in Section 2, after prediction a new point by Bayesian filter, to reduce error it should be updated by measurement stage in order to reduce error. So far, several methods have been proposed for measurement stage of Bayesian filters [11], [12], where dependency to road gray level is the main challenge. As, the gray level of some regions may not have standard homogeneity, increase the gray level variance may occur the measurement area. In this paper, in order to overcome the mentioned problem, both radiometric (by using the road grey level) and geometric features (edge detection) features are used.

Finding a proper measurement point has two stages. At first (using radiometric features) the smooth image shown in Fig. 2(b) is used. We move forward according to previously measured angle of the road (step k-1) with the scale of dt (as shown in Fig. 7(a)) to find a new road point candidate, (r'_k, c'_k) is,

$$\begin{aligned} r'_k &= r_{k-1} - dt\,\sin(\theta_{k-1}) \\ c'_k &= c_{k-1} + dt\,\cos(\theta_{k-1}) \end{aligned} \qquad (27)$$

where (r'_k, c'_k) is the road point candidate, (r_{k-1}, c_{k-1}) is the road point coordinate at stage *k-1*, and dt is the distance between two points. Sample profile, **spf** , is obtained according to the candidate road point (r'_k, c'_k) , then matching error is determined according to Eq. 22. If the profile matching error is less than 0.2, the candidate road point is used for stage two of measurement processing, otherwise searching for another candidate road points is continued by considering interval $\theta_k = \theta_{k-1} - \frac{1(radian)}{2} : \theta_{k-1} + \frac{1(radian)}{2}$ for measured road angle with step equals 0.08 radian.

At the second stage (using geometric features) the edge image shown in Fig. 2(d) is used. The SWO is placed on the candidate road point (see Fig. 7(b)), some spokes that crosses two edges (see Fig. 7(c)) is considered as the spoke candidate group, and the spoke with minimum length is chosen as the main spoke (see Fig. 7(d)).

The candidate point is moved along the spoke to the center, and it is supposed as the measuring coordinates (see Fig. 7(e)). The measuring, θ_k also obtained,

$$\theta_k = \tan^{-1}\left(\frac{r_k - r_{k-1}}{c_k - c_{k-1}}\right) \qquad (28)$$

The road width is an effective parameter in road tracking algorithm. The accuracy of the road can be realized through the width. Moreover, it benefits Bayes algorithm in placing the candidate point in the center. By using the new road point, (r_k, c_k) , both road width and reference are updated. The road width is the minimum length of that spoke crosses two edges where SWO is placed on the road point.

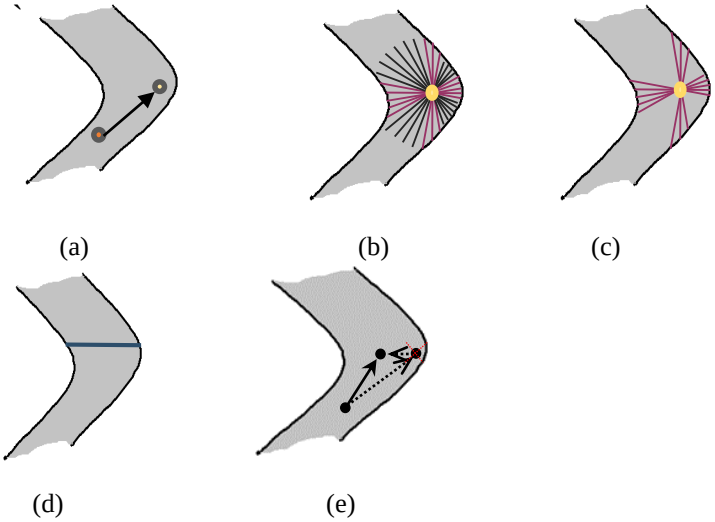

Fig. 7. Finding a candidate for the step k according to the road in the previous step *k-1* and the angle of the road (a) find the best candidate point (b) insert SWO on candidate point (c) spokes is removed if edge of road is not cut (d) Selecting the best candidate for spoke (e) Selecting the best point for measuring.

Moving ahead, road features consists of road width, gray levels and edges change. So when the reference profile is assumed always stable along the road, the result from profile matching method (refer to Eq. 22) cannot be trusted in case of alterations in road features. Therefore, updating the reference profile is necessary at every measurement stage. To perform that task, we initially follow the method explained in Section 3.1.2 .

In addition the width might change along the road and having a stable reference profile length, will decrease accuracy of the process. For instance, when the width is too little or even less than length of reference profile, L_{rpf} , no more pixels will be detected to road candidate. Or when it is too huge, more than the length of reference profile, it will decrease the accuracy of choosing the best point to road candidate. To organize the number of elements in reference profile, we should first get the road width at step k and use this reference profile in processing of later steps. (refer to Eq. (1^{V}))

The scale parameter, dt , should be considered along moving through the road direction. Under presumption dt small, the processing would be time consuming and under presumption dt large, either a pixel out of the road may be candidate or no point find. In this paper, two values for scale parameter is used, i.e. $dt = \frac{b_k}{3s}$ and $dt = \frac{b_k}{6s}$. To enhance the processing speed high scale is used, $dt = \frac{b_k}{3s}$, and The small scale value $dt = \frac{b_k}{6s}$ is used when the difference between θ_k and θ_{k-1} exceed, car block, or no point is found.

IV. Experiment and Result

A. Study Area

In this Section, we are going to track the roads of two SAR images. The first image, shown in Fig. 10(a) is a digital orthophoto quads (DOQ) and the second SAR image, shown in Fig. 11(a). The first image shows Marietta, Florida in America and the second SAR image shows the Kish Island in Iran.

The DOQs are orthogonally rectified images produced from aerial images taken at height of 20,000 ft, with an approximate scale of 1:40,000 and a ground resolution of 1 m. The image included scenes from trans-national highway, intra-state highway and roads for local transportation. Furthermore, they have contained different road types, such as straight road, curves, ramps crossing and bridge. The image contains various road conditions, including occlusion by vehicles, trees and shadows.

The Kish island SAR image is from high resolution satellite image tested on multi-spectral Ikonos image, and it makes by using the 1:8000 scale, and roads have variable width which it is between 8 to 16 pixels. This image contains one square and many junctions.

B. Evaluation Criteria

In general, the performance comparisons of road detectors and trackers is not an easy task because they may use different imagery or different sources. In this paper, the evaluation framework introduced in [22] is adopted, in terms of completeness, correctness and quality. The extracted roads were compared with reference roads (as ground truth), which are generated from the road vector data from the Graphic Information System (GIS), are adopted to evaluate the quality of road extraction. These measures are defined as follows:

Completeness [22] is defined as the percentage of the reference data which was detected during road extraction

$$\text{Completeness} = \frac{\text{Length of matched reference}}{\text{Length of reference}} \tag{29}$$

Length of matched reference is the road pixels obtained by an extraction algorithm which is coinciding with the length of reference data. The length of reference road is obtained by using the ground truth (reference road) maps. The image for completeness parameter is [0, 1] where the optimal value equals "1" means 100% of roads are detected.

correctness [22] represents the percentage of the extracted road data which is correct:

$$\text{Correctness} = \frac{\text{Length of matched extraction}}{\text{Length of extraction}} \tag{30}$$

Length of extraction is total extraction point which is contained of the matched and unmatched extraction point to the reference road points (ground truth). The range value for correctness is [0, 1], where the optimal value equals "1" which means in which case 100% of the extracted roads are actual roads.

Quality [22] is used for goodness measuring of the final result.

$$\text{Quality} = \frac{\text{Length of matched extraction}}{\text{Length of extraction+Length of unmatched reference}} \tag{31}$$

Length of unmatched reference is the road pixels which are in the reference data but not in the obtained result. Meanwhile as seen in Eq. 31, the quality parameter is affected by two aforementioned parameters, completeness and correctness.

C. Test Area

As observed in the context, several stable sums which are presumed for threshold, system and measurement error covariance matrix are discussed below:

$$\mathbf{Q_k} = \begin{bmatrix} 0.04W & 0 & 0 & 0 \\ 0 & 0.04W & 0 & 0 \\ 0 & 0 & 0.02 & 0 \\ 0 & 0 & 0 & 0.01 \end{bmatrix} \tag{32}$$

$$\mathbf{R_k} = \sigma_{\varphi}^2 \begin{bmatrix} 0.4W & 0 & 0 \\ 0 & 0.4W & 0 \\ 0 & 0 & 1 \end{bmatrix} \quad (33)$$

$$b_{\max} = \frac{6 \times 4}{resolution}$$

(For 6 lanes of road and length of each lane is 4-meters)

T_{line} =max of building length / resolution

Marietta, Florida is shown in Fig. 10. As well shown, most area of the road is detected. One of the advantages of our method compared to other tracking methods is feedback and automation algorithms. For example as can be seen in the upper part of Fig. 10, Because of the dense trees the tracking algorithm by using the EKF or PF in an area of the road is not able to continue working, and tracking the road continues by using the automatically finding the other initial point and this is one of the advantages of our method. As well as shown is Table. 1 our test image result have a 95% correctness, 98% completeness and 94% quality and compared with Method …. And …, better results are obtained. Only part of the road which is located in the southern part of the image haven not been identified, because of very heterogeneous surfaces and Northeastern part of the image is detected that is wrong.

In the second image Kish island in Iran were tested that the performance of our algorithm is shown on this image whereas after road extraction of an image that contains a field and several junctions, we got very good result and correctness is 100%, meanwhile completeness and quality is 99%, because of this result, we are indebted to initial proper pre-processing and remove points that will cause an error in processing. Meanwhile in this image, we are not need to feedback and finding new point for reprocessing and roads is detected in a processing.

Table 1 : comparison of the road extraction results

	Completeness	Correctness	Quality
C. Poullis [23]	83	66	58
M. Negri [24]	76	63	59
CH. He [25]	74	76	60
Florida(Fig. (9)**)**	98	95	94
Kish Island(Fig. (10)**)**	99	100	99

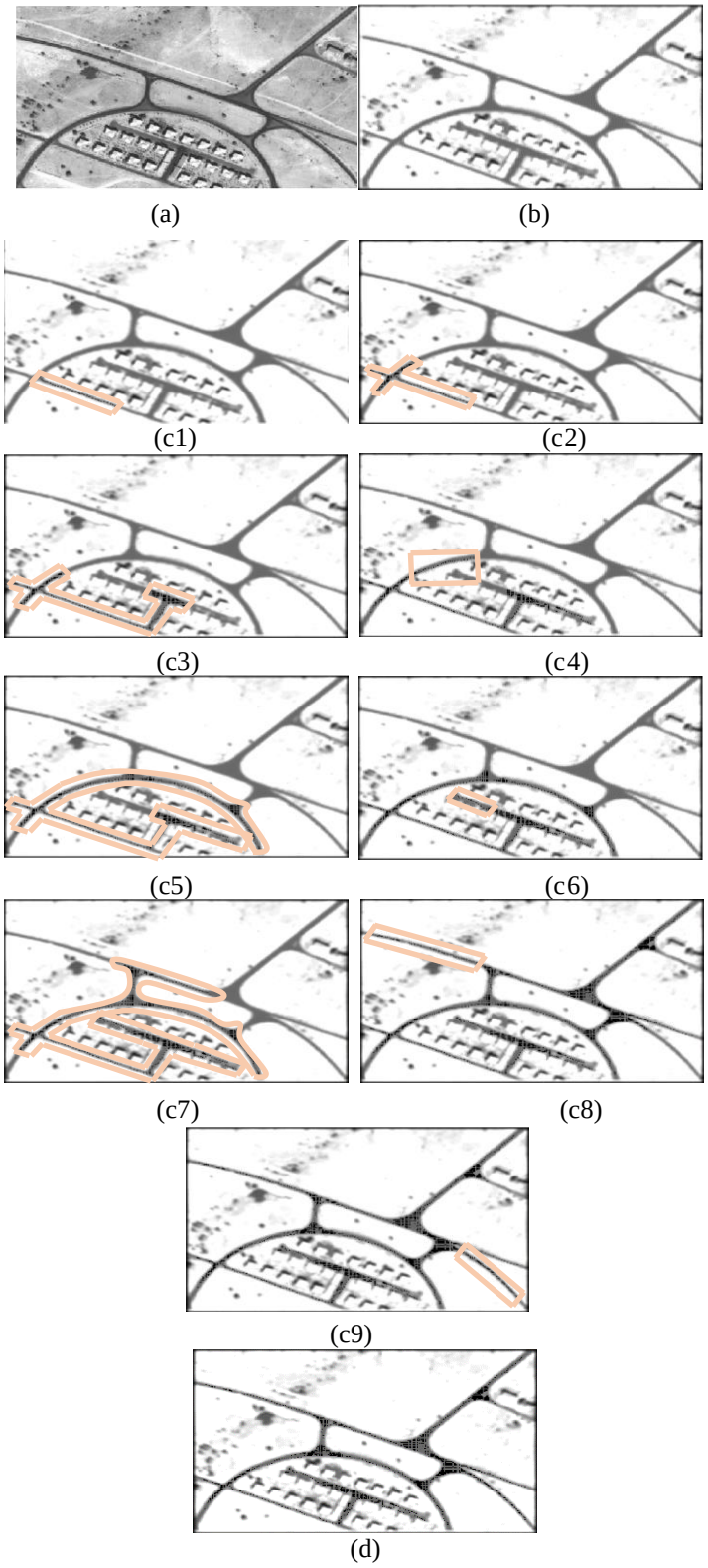

Fig. 9. : (a) Quickbird satellite image (b) The image of the mask LOG /c1~c9/ automatic find the road by using EKF and PF (d) final image that roads are shown.

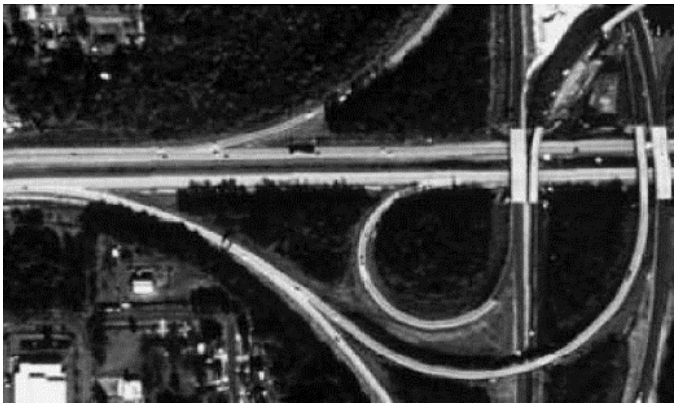

(a)

(b)

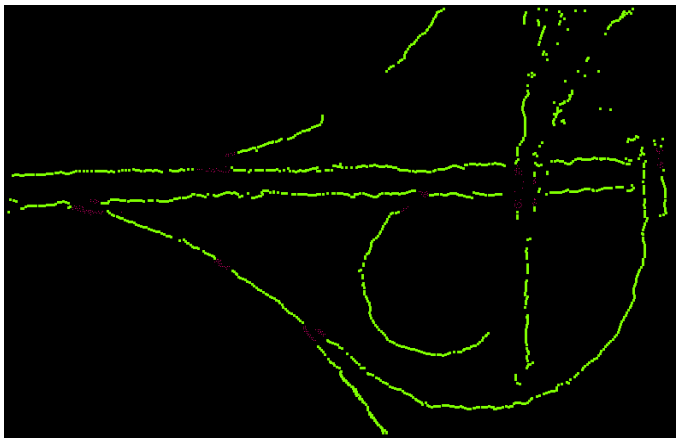

(c)

Fig. 10. (a) An image sample extracted from DOQ (b) image with extracted road (c) extracted road.

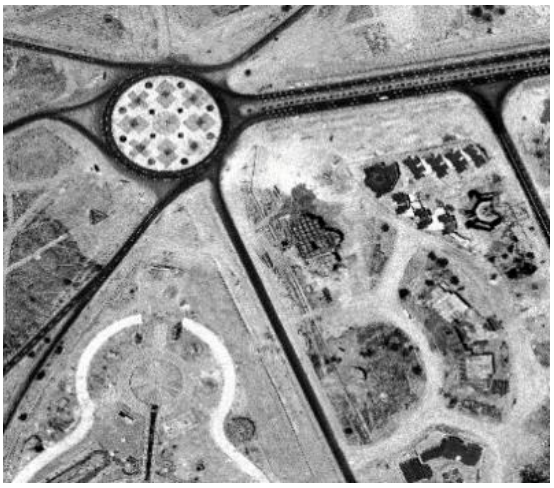

(a)

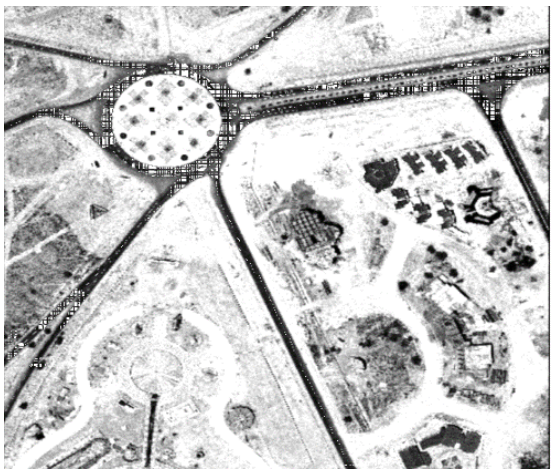

(b)

Fig. 11. (a) Original image (b) image with extracted road

V. CONCLUSION

In this paper for the first time, with the use of Bayesian filters, we automatically extracted roads from SAR imagery. First, initial coordinates, width, angle and profile are identified automatically. Then, straight, curved or slightly blocked ones are tracked by using EKF and when the tracking reaches severe blockage or junctions, the former algorithm stops and the processing is continued by using the PF. After several steps in PF and clustering the positioned samples, the ultimate pixel from each cluster is delivered to EKF and tracking move Forward through EKF. This recursive algorithm continues until tracking reached a dead-end and stops. In this paper, measuring Section of Bayesian filter has been improved over methods [11] and [12] in order to enhance accuracy of the algorithm. Edge-finding and profile matching algorithms are used simultaneously.

Later in this essay, images from Kish Island, Quickbird Sat, and an image from the height of *20000ft* were operated on and mostly were tracked accordingly.
The algorithms used here are related to accuracy and speed, and there is room for improvement in all of them in the future. Among the solutions for maximizing the speed of tracking by using the Bayesian filter, we should consider improving preprocessing Section *i.e.* applying a more efficient method in tresholding. Also, to enhance accuracy, regulable PF(RPF) [16] and Kalman filter unscented [15] can be great assets.

VI. Reference

[1] R. Bajcsy and M. Tavakoli, "Computer recognition of roads from satellite pictures," IEEE Trans. Syst., Man, Cybern., vol. SMC-6, no. 9, pp. 623–637, Sep. 1976.

[2] Y. T. Zhou, V. Venkateswar, and R. Chellapa, "Edge detection and linear feature extraction using a 2-D random field model," IEEE Trans. PatternAnal. Mach. Intell., vol. 11, no. 1, pp. 84–95, Jan. 1989.

[3] J. Canny, "A computational approach to edge detection," IEEE Trans. Pattern Anal. Mach. Intell., vol. PAMI-8, no. 6, pp. 679–698, Nov. 1986.

[4] Silvia Valero *et al* "Advanced directional mathematical morphology for the detection of the road network in very high resolution remote sensing images". Pattern Recognition Letters 31(10): 1120-1127 (2010)

[5] D. M. McKeown and J. L. Denlinger, "Cooperative methods for road tracking in aerial imagery," in Proc. CVPR, 1988, pp. 662–672.

[6] J. Zhou, W. F. Bischof, and T. Caelli, "Road tracking in aerial images based on human computer interaction and Bayesian filtering," ISPRS J.Photogramm. Remote Sens., vol. 61, no. 2, pp. 108–124, 2006.

[7] R. Huber and K. Lang, "Road extraction from high-resolution airborne SAR using operator fusion," in Proc. IEEE Int. Geosci. Remote Sens.Symp., 2001, vol. 6, pp. 2813–2815.

[8] P. Gamba, F. Dell'Acqua, and G. Lisini, "Improving urban road extraction in high-resolution images exploiting directional filtering, perceptual grouping, and simple topological concepts," IEEE Geosci. Remote Sens.Lett., vol. 3, no. 3, pp. 387–391, Jul. 2006.

[9] W. Shi and C. Zhu, "The line segment match method for extracting road network from high-resolution satellite images," IEEE Trans. Geosci.Remote Sens., vol. 40, no. 2, pp. 511–514, Feb. 2002.

[10] M. Barzohar and D. B. Cooper, "Automatic finding of main roads in aerial images by using geometric stochastic models and estimation," IEEE Trans. Pattern Anal. Mach. Intell., vol. 18, no. 7, pp. 707–721, Jul. 1996.

[11] Sahar Movaghati, Alireza Moghaddamjoo, Ahad Tavakoli: Road Extraction From Satellite Images Using Particle Filtering and Extended Kalman Filtering. IEEE T. Geoscience and Remote Sensing 48(7): 2807-2817 (2010)

[12] G. Vosselman and J. Knecht, "Road tracing by profile matching and Kalman filtering," in Automatic Extraction of Man-Made Objects FromAerial and Space Images. Basel, Switzerland: Birkhuser Verlag, 1995,

[13] J. Zhou, W. F. Bischof, and T. Caelli, "Robust and efficient road tracking in aerial images," in Proc. Joint Workshop ISPRS and DAGM(CMRT) Object Extraction 3D City Models, Road Databases TrafficMonitoring Concepts, Algorithms Evaluation, Vienna, Austria, 2005,pp. 35–40.

[14] F. Tupin, *et al* "Detection of linear features in SAR images: Application to road network extraction," IEEE Trans. Geosci. Remote Sens., vol. 36, no. 2, pp. 434–453, Mar. 1998.

[15] Sahar Movaghati, Alireza Moghaddamjoo, Ahad Tavakoli "Using Unscented Kalman Filter for Road Tracing from Satellite Images. " Asia International Conference on Modelling and Simulation 2008: 379-384

[16] Oudjane, N , Musso, C. "Progressive correction for regularized particle filters," IEEE Transactions on Information Fusion, 2000. FUSION 2000. Proceedings of the Third International Conference ,THB2/10 - THB2/17 vol.2

[17] E.A. Carvalho, "SAR imagery segmentation by statistical region growing and hierarchical merging " : Digital Signal Processing 20 (2010) 1365–1378

[18] A. P. Dal Poz *et al* "Semi-Automatic road extraction by dynamic programming optimization in the object space: single image case," The International Archives of the Photogrammetry, Remote Sensing and Spatial Information Sciences of ISPRS 2008, Vol. 34

[19] J. Hu, *et al* "Progressive correction for regularized particle filters," IEEE Transaction on GEOSCIENCE and REMOTE SENSING, vol. 45, NO. 12, December 2007

[20] N. Otsu, "A threshold selection method from gray-level histogram," IEEE Transactions on System Man Cybernetics, Vol. SMC-9, No. 1, 1979, pp. 62-66.

[21] L. Bay "Road tracking using particle filters with partition sampling and auxiliary variables" Computer Vision and Image Understanding, Volume 115, Issue 10, October 2011, Pages 1463–1471

[22] Wiedemann, C. Hinz "Delineation and geometric modeling of road networks" International Archives of Photogrammetry, Remote Sensing and Spatial Information Sciences 32 (Part 3/2W5), 95-100.

[23] C. Poullis, S. You "Automatic extraction and evaluation of road networks from satellite imagery" ISPRS Journal of Photogrammetry and Remote Sensing 65 (2010) 165-181.

[24] M. Negri, *et al* "Junction-Aware Extraction and Regularization of Urban Road Networks in High-Resolution SAR Images" IEEE Transaction on geoscience and remote sensing, Vol. 44, No. 10, October 2006.

[25] CH. He, *et al* "Road Extraction from SAR Imagery Based on Multiscale Geometric Analysis of Detector Responses" IEEE Journal of selected topics in applied

earth observation and remote sensing, Vol. 5, No. 5, October 2012.

[26] R. O. Duda, P. E. Hart, and D. G. Stork "Pattern Classification" 2nd ed. New York: Wiley-Interscience, 2000.

[27] "Standard specification for construction of roads and bridges on federal highway projects" U.S. Department of Transportation, Federal Lands Highway 2014.